High Pressure Vibrational and Polymorphic Response of 1,1-Diamino-2,2-Dinitroethene (FOX-7) Single Crystals: Raman Spectroscopy.

ARTICLE *in* THE JOURNAL OF PHYSICAL CHEMISTRY A · JUNE 2014

Impact Factor: 2.69 · DOI: 10.1021/jp5052062 · Source: PubMed

3 AUTHORS, INCLUDING:

Zbigniew Dreger
Washington State University
124 PUBLICATIONS **1,127** CITATIONS

SEE PROFILE

Yuchuan Tao
Florida State University
14 PUBLICATIONS **64** CITATIONS

SEE PROFILE

THE JOURNAL OF PHYSICAL CHEMISTRY A

Article

pubs.acs.org/JPCA

High-Pressure Vibrational and Polymorphic Response of 1,1-Diamino-2,2-dinitroethene Single Crystals: Raman Spectroscopy

Zbigniew A. Dreger,* Yuchuan Tao, and Yogendra M. Gupta

Institute for Shock Physics and Department of Physics and Astronomy, Washington State University, Pullman, Washington 99164-2816, United States

Supporting Information

ABSTRACT: Raman spectroscopy was used to examine the vibrational and polymorphic behavior of 1,1-diamino-2,2-dinitroethene (FOX-7) to elucidate its structural and chemical stability under high pressure. Measurements were performed on single crystals compressed in a diamond anvil cell, and data were obtained over the entire frequency range of FOX-7 Raman activity. Several new features were observed with increase of pressure: (i) new vibrational peaks and discontinuity in the shifts of the peaks at 2 and 4.5 GPa, (ii) apparent coupling or mixing of several modes, and (iii) changes in the NH_2 stretching spectral shape and modes shift. The spectral changes at 2 GPa, in contrast to previous reports, involved only a few peaks and likely resulted from a small molecular transformation. In contrast, changes at 4.5 GPa involved most of the modes, and the pressure for the onset and completion of the changes depended on the pressure medium. A large pressure hysteresis regarding the changes at 4.5 GPa implies a reconstructive transformation. We suggest that this transformation reflects a change in the balance between interlayer (van der Waals) and in-layer (H-bonding) interactions. Despite these transformations, further compression to 40 GPa and subsequent release of pressure did not cause any irreversible changes. This finding implies that FOX-7 has remarkable chemical stability under high pressures. The observed coupling between the various modes with increasing pressure was analyzed within the Fermi resonance model. The potential implication of the coupling of modes for shock insensitivity of FOX-7 is briefly discussed.

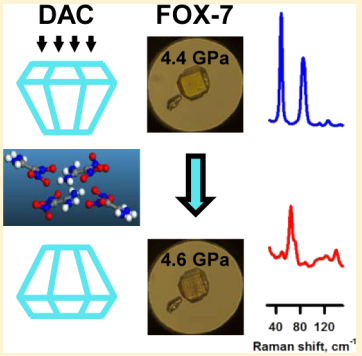

1. INTRODUCTION

1,1-Diamino-2,2-dinitroethene (commonly known as FOX-7) is a relatively new, high-performance, and low-sensitivity high explosive (HE) crystal. Because of the continuing strong interest in developing safer high explosives, the low sensitivity to initiation (e.g., by shock, impact, friction, or heat) of FOX-7 has attracted considerable interest.[1−9] However, the microscopic factors that govern the low sensitivity are not well-understood. To address this need, a good understanding of the molecular mechanisms in FOX-7 is required at the conditions of interest. Because of the interest in understanding shock wave initiation of FOX-7, high-pressure and high-temperature (HP-HT) conditions relevant to shock wave compression are of particular interest.

Shock wave induced initiation or decomposition of HE crystals requires energy transfer to the molecules in the crystal. Although the energy transfer mechanisms have not been established, it is recognized that vibrational properties of both the crystal lattice and the individual molecules likely play an important role in this process, e.g., see ref 10. Thus, a careful examination of both intramolecular and lattice vibrations of FOX-7, under extreme conditions, is needed to understand its low sensitivity. Furthermore, vibrational studies are important for examining polymorphic transformations at extreme conditions. Because different polymorphs of the same explosive can have different molecular conformations and/or intermolecular arrangements, a good knowledge of the polymorphic phases is important for understanding the reactive behavior of shock-compressed HEs.

In our work, we have used Raman spectroscopy to examine the vibrational structure of FOX-7. Raman spectroscopy has proved to be a versatile method for elucidating the vibrational and polymorphic behavior of HE crystals under extreme pressures and/or temperatures.[11−15]

At ambient conditions, FOX-7 crystallizes in a monoclinic structure with a space group of $P2_1/n$.[2] As shown in Figure 1, the FOX-7 unit cell is occupied by four molecules. The molecules are arranged "head-to-tail", forming wave-shaped layers in the (101) plane with extensive intra- and intermolecular hydrogen bonding within the layers; specifically, there are 2 intra- and 12 intermolecular hydrogen bonds. The layers are separated by ∼0.31 nm and held together by van der Waals forces. Previous studies have demonstrated that the ambient structure (α-FOX-7) transforms to other two polymorphs, β and γ, at higher temperatures.[16−18] The transitions to new polymorphs were reported to occur above ∼386 K (α–β) and ∼446 K (β–γ). The β- and γ-polymorph structures were determined to be the $P2_12_12_1$ and $P2_1/n$, respectively. An increase in the displacement of nitro groups out of the molecular plane was associated with both

Received: May 27, 2014
Revised: June 17, 2014
Published: June 18, 2014

   dx.doi.org/10.1021/jp5052062 | J. Phys. Chem. A 2014, 118, 5002−5012

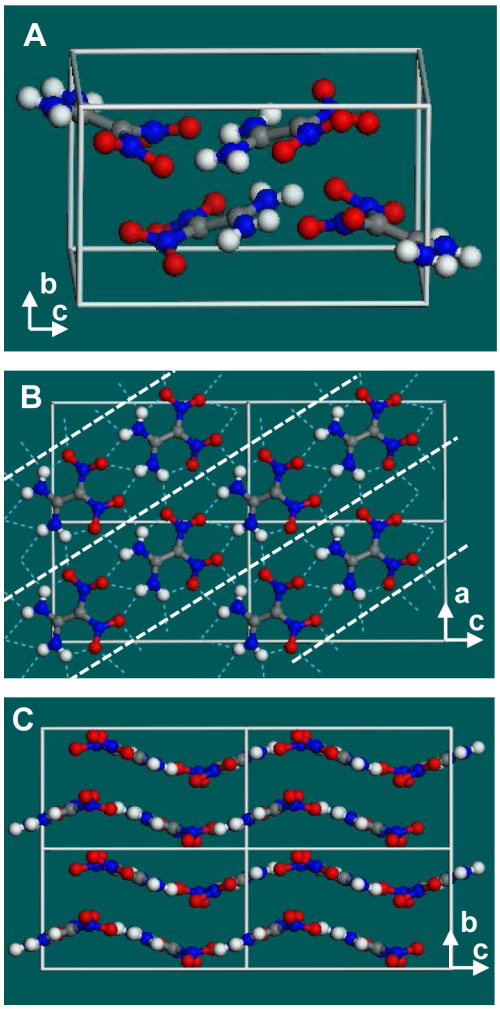

Figure 1. Crystal structure of FOX-7 at ambient pressure: (A) unit cell; (B) projection of structure on the (101) plane, showing arrangement of molecules in the layer; (C) projection of structure on the (011) plane, showing arrangement of wave-shaped layers. The white-dashed lines mark "the bands" of the head-to-tail arrangement of molecules in the layer. Molecules are represented by the ball-and-stick model. Hydrogen bonds are denoted by blue dashed lines. Legend: carbon, gray; nitrogen, blue; oxygen, red; hydrogen, white. Crystal unit cells are represented by white lines.

transformations. The $\alpha-\beta$ transition was reversible, whereas the $\beta-\gamma$ was partially reversible.[17,18]

The high-pressure response of FOX-7 is not well-established, and contradictory results have been reported.[19−23] Peiris et al.[19,20] reported Raman and X-ray diffraction studies on powder samples to ∼8 GPa. Using NaCl or no pressure-transmitting medium, they observed changes in the Raman spectra and X-ray diffraction patterns at ∼1.0 GPa and above 4.5 GPa. The changes at 1.0 GPa were associated with an unspecified phase transformation, whereas the changes at 4.5 GPa were ascribed to amorphization and/or decomposition. In contrast, IR experiments with FOX-7 powder mixed with KBr indicated spectral changes around 2, 5, or 6 and 10 GPa.[21,22] However, no amorphization or decomposition was observed up to 28 GPa.[21] Furthermore, it was suggested[22] that the spectral changes at 2 and 6 GPa can correspond to the temperature-induced $\alpha-\beta$ and $\beta-\gamma$ transitions, respectively.

Unlike the previous studies on FOX-7 powders, we obtained Raman measurements on single crystals to 15 GPa and observed spectral changes at 2 and 4.5 GPa.[23] Contrary to the suggestion in ref 22, we demonstrated that the high-pressure and high-temperature phases are different.[23]

Results from computational studies are also contradictory. Using density functional theory (DFT) calculations, no phase transitions were revealed for compression to 100 GPa.[24] In contrast, recent calculations suggested numerous phase transitions: at 2, 5, 11, 19, 29, and 35 GPa.[25] The contradictory results to date do not provide a good basis for understanding the behavior of FOX-7 under high pressures. Potential shortcomings in experimental and computational methods likely contribute to these inconsistencies.

It is generally recognized that high-pressure results can be affected by sample quality and variations in pressure-transmitting media. For example, the random morphology of polycrystalline samples, grain interactions under pressure, and uncertain compression conditions due to a lack of pressure-transmitting medium can distort pressure effects in molecular solids. To overcome these shortcomings, the experiments reported here were performed with good quality single crystals and under controlled pressure loading.

The present work builds on our previous brief report[23] and provides, for the first time, comprehensive results on changes in the Raman spectra of FOX-7 over a broad range of frequencies and pressures. In contrast to the previous studies,[19−22] our experiments provide spectra with high spectral resolution and results on lattice vibrations. The specific objectives of this work were (i) to examine high-pressure structural and chemical stability, (ii) to determine changes in both intramolecular and lattice vibrational modes under high pressure to identify the factors that may destabilize the ambient structure, (iii) to ascertain changes in hydrogen bonding, and (iv) to examine previous conjectures regarding the phase transitions. The present study also provides comprehensive experimental results for future theoretical studies on vibrational and polymorphic structures of FOX-7.

The remainder of the paper is organized as follows. Experimental procedures, including sample preparation, high-pressure generation, and Raman measurements, are described briefly in the next section. Section 3 presents experimental results and discussions regarding (i) pressure dependence of intermolecular and lattice vibrations to 40 GPa, (ii) changes in hydrogen bonding, (iii) polymorphic transformations, and (iv) vibrational coupling. The main findings of this work are summarized in Section 4.

2. EXPERIMENTAL METHODS

Polycrystalline FOX-7, in powder form, was obtained from Dr. Joel R. Carney of the Naval Surface Warfare Center−Indian Head Division (NSWC-IHD). Single crystals were grown from a solution of FOX-7 in dimethyl sulfoxide (DMSO) at room temperature. Typical crystals had rectangular shapes with well-developed faces either normal or parallel to the *b*-axis. The crystals were used as grown, but they were selected on the basis of crystal quality and size to fit the high-pressure compartment.

High pressures were generated using a modified Merrill-Bassett type diamond-anvil-cell (DAC). A rhenium gasket, preindented to 0.05 mm with a 0.12 mm hole drilled in the indentation, served as the sample compartment. Most experiments were performed using cryogenically loaded nitrogen as a pressure-transmitting medium. We verified that cryogenic loading did not affect the crystal quality. Occasionally, cryogenically loaded argon or methanol (M) and ethanol (E)

dx.doi.org/10.1021/jp5052062 | J. Phys. Chem. A 2014, 118, 5002−5012

mixture (M/E: 4/1) were also used as pressure-transmitting media. Frequency shifts of the ruby R-lines were used to monitor pressure in the sample compartment. The precision of our pressure measurements was estimated to be 0.05 GPa.

The 532 line from a cw diode-pumped solid-state laser was used for Raman excitation. A micro-Raman system (T64000, JY-Horiba) equipped with a microscope (Olympus BX-40) was used; it provided a spectral resolution of ~0.8 cm^{-1} and a spatial resolution of 5 μm. The system was capable of measuring spectra to frequencies as low as 20 cm^{-1}. Less than 1 mW of power was used to avoid any damage to the sample. The single crystals used in these studies were oriented such that the *b*-axis was either parallel or perpendicular to the direction of the excitation beam. The orientation of crystals was determined on the basis of the known cleavage plane. Raman spectra measurements were performed up to 40 GPa. Pressure-induced shifts of overlapping peaks were analyzed by fitting the spectra to a Voigt (Gaussian−Lorentzian) function using a nonlinear least-squares algorithm. Experimental details regarding our Raman and ruby fluorescence techniques can be found elsewhere.[12,14,26]

3. RESULTS

3.1. Raman Spectra at Ambient Pressure. The FOX-7 molecule possesses C_2 point group symmetry.[2] Thus, the irreducible representations for the free molecule vibrations (14 atoms) assumes the form $\Gamma_{int} = 18A + 18B$. In the crystal, the four FOX-7 molecules are distorted and located on the C_1 sites in the unit cell.[2] Taking into account the factor group symmetry of FOX-7 (C_{2h}), the C_1 site can be mapped onto the unit cell to obtain the symmetries of the internal (intramolecular) and external (lattice) vibrations in the crystal in the following forms: $\Gamma_{int} = 36A_g + 36B_g + 36A_u + 36B_u$ and $\Gamma_{ext} = 6A_g + 6B_g + 5A_u + 4B_u$. Only the even parity (g) vibrations are Raman-active. Thus, one expects to observe 12 lattice modes and 72 intramolecular modes in the Raman spectra. However, because of a weak crystal field, the Davydov-split components of the originating molecular transitions are not easy discernible and only 36 intramolecular modes are expected to be observed.

In Figure 2, we present the Raman spectra of FOX-7 over a broad frequency range that includes, for the first time, lattice and NH_2 stretching vibrations. The spectra were obtained using

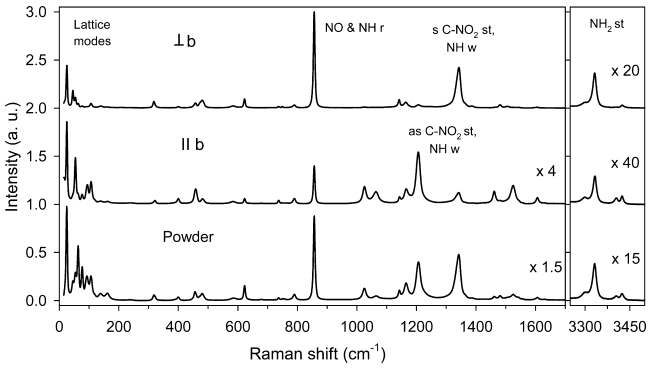

Figure 2. Raman spectra of single-crystal and powder samples of FOX-7. Single-crystal spectra were obtained for two orientations: *b*-axis normal or parallel to the laser beam direction. Tentative assignments for the selected, high-intensity peaks are indicated. Spectra intensities are normalized to the intensity of the 856 cm^{-1} peak in the top spectrum (*b*-axis normal to the laser beam direction).

both single-crystal and polycrystalline samples; the single-crystal spectra were measured with the laser beam either normal or parallel to the crystal *b*-axis. A comparison of the spectra reveals significant effects of crystal orientation on both the absolute and relative intensities of various Raman peaks, confirming the strong crystallographic anisotropy of FOX-7 observed in X-ray diffraction studies.[2]

The Raman frequencies obtained from the spectra (Figure 2) are presented in Table 1, along with their tentative vibrational assignments adopted from refs 20 and 27. To distinguish between intramolecular and lattice modes, we utilized the vibrational scaling law (VSL) that was used previously for molecular crystals.[14,28] On this basis, we determined that peaks located below ~170 cm^{-1} can be assigned as lattice modes. Overall, we were able to detect 10 lattice and 36 intramolecular modes. From the latter, 27 modes were assigned to fundamental vibrations and 9 modes to combinations or overtones. In Table 1, we also compared our results with the only published Raman data.[20] Although the previous study provided a very limited number of Raman peaks, good agreement is observed between the two sets of data.

Before presenting pressure-induced changes in the Raman spectra (intensities and peak shifts) we note the following. Because the intensity, absolute and relative, of the peaks depends on the crystal orientation, high-pressure experiments were performed for both crystal orientations shown in Figure 2. This approach allowed us to determine the pressure shift for all accessible FOX-7 Raman modes.

3.2. Pressure Effects on Raman Modes. *3.2.1. Frequency Range 0−1300 cm^{-1} (Contributions from Lattice, NH and NO Wagging and Rocking, and C−NO_2 Vibrations).* The results in this frequency range are presented in Figures 3 and 4. Figure 3 shows the Raman spectra at several pressures, while Figure 4 displays the pressure shifts of the Raman peaks. The spectra in Figures 3 were obtained with the laser beam parallel to the *b*-axis of the crystal. With increasing pressure, several spectral features are observed: (i) blue shift of the peaks; (ii) new pattern of the peaks at 5.1 GPa; (iii) decrease in intensity of the peaks at 5.1 GPa, especially in the lattice modes (the intensity of the spectra at 5.1 GPa and at higher pressures were multiplied by 2); (iv) gradual increase in the spectra intensity with pressure increase from 5.1 to ~30 GPa; and (v) broadening of peaks and a decrease of their intensities above ~30 GPa. Despite all of these pressure-induced changes, the intensity and the pattern of the peaks were fully reversible after a complete release of pressure; see for comparison the top and bottom spectra in Figure 3. This result shows that neither the pressure increase to 40 GPa (highest pressure reached in this work) nor the subsequent release of pressure to 1 atm caused any measurable irreversible changes. The chemical stability of FOX-7 over such a large range of pressure is quite remarkable for a molecular crystal and is in accord with its low sensitivity.

The results presented in Figure 4 reveal several characteristic features associated with pressure shifts: (i) shifts for lattice modes larger than those for intramolecular modes, (ii) changes in shifts of several modes around 2 GPa, (iii) significant changes in shifts of numerous modes around 4.5 GPa, and (iv) apparent interaction or coupling of some modes located at 700−900 cm^{-1}.

To quantify changes in the vibrational modes, pressure dependences of the Raman shifts ($d\nu/dp$, pressure coefficient) were determined from the least-squares fits of the experimental data to quadratic polynomials. The calculated coefficients are

dx.doi.org/10.1021/jp5052062 | J. Phys. Chem. A 2014, 118, 5002−5012

Table 1. Frequencies and Pressure Coefficients ($d\nu/dp$) of Raman Modes of FOX-7 at Ambient and Transition Pressures[a]

	freq at 1 atm or at the transition			$d\nu/dp$ (cm^{-1} GPa^{-1})		
mode	this work (cm^{-1})	ref. (cm^{-1})	tent. vibr. assign.	α (1 atm)	I (2 GPa)	II (5 GPa)
L_1	25		lattice	7.2	5.3	3.4
L_2	46		lattice	13.3	8.9	
L_3	54		lattice	11.1	7.3	5.0
L_4	63		lattice	8.7	6.0	
L_1^{II}	64 (5)					4.8
L_2^{II}	71 (5)					4.9
L_5	77		lattice	11.5	8.1	8.6
L_6	90		lattice	12.7	8.4	7.2
L_7	98		lattice	16.5	11.0	7.4
L_8	107		lattice	12.4	11.4	9.9
L_9	139		lattice	18.4	14.3	
L_1^{I}	151 (2)				11.9	10.3
L_3^{II}	159 (5)					6.2
L_{10}	162		lattice	18.3	16.1	12.7
L_4^{II}	220 (5)					11.5
L_5^{II}	231 (5)					10.2
ν_1	246		ool H w[b]	7.7	7.3	4.9
ν_2	318	320	ool H w[b]	6.9	6.0	
ν_1^{II}	374 (5)					3.4
ν_2^{II}	391 (5)					4.4
ν_3	400	400	il as NH w[b]	4.9	3.9	3.7
ν_3^{II}	447 (5)					2.7
ν_4	457	460	il s NH w[b]	6.2	3.6	2.6
ν_5	472		skeletal breathe[c]	7.0	5.6	3.5
ν_6	481	480	s NO and NH w[b]	9.7		5.3
ν_7	583		s NH w, C−C st[b]	8.5	6.2	
ν_1^{I}	607 (2)				9.0	3.8
ν_8	622	622	ool s NH w[b]	3.9	3.1	
ν_4^{II}	681 (5)					7.6
ν_5^{II}	695 (5)					1.7
ν_6^{II}	709 (5)					6.4
ν_9	737		ool s NO w[b]	1.5	0.8	
ν_{10}	749		ool CN w[b]	0.9	0.7	
ν_7^{II}	767 (5)					1.4
ν_{11}	789	790	C−NO_2 r[c]	−1.8	0.5	1.4
ν_8^{II}	794 (5)		2 ν_2^{II}			4.4
ν_{12}	856	860	NO and NH r[b]	2.0	1.7	1.6
ν_{13}	1024	1025	il as NH w[b]	0.6	0.9	−1.7
ν_{14}	1070	1065	il s NH w[b]	4.8	3.0	2.2
ν_{15}	1142	1142	C−NO_2 w, as NH w[b]	4.3	2.8	3.1
ν_{16}	1165	1165	C−C st, NH w[b]	0.6	1.8	3.1
ν_{17}	1208	1210	as C−NO_2 st, NH w[b]	2.6	2.9	4.3
ν_{18}	1311		$\nu_4 + \nu_{12}$	1.8	1.8	2.0
ν_{19}	1336		$\nu_6 + \nu_{12}$			3.3
ν_{20}	1343	1342	s C−NO_2 st, NH w[b]	4.9	4.6	4.2
ν_{21}	1364		$\nu_8 + \nu_9$	1.3	4.0	
ν_{22}	1386		s C−NO_2 st[c]	4.2	3.0	6.7
ν_{23}	1464		C−C st, NH w[b]	0.7	1.0	−0.9
ν_{24}	1481		$\nu_8 + \nu_{12}$	0.9	0.6	1.4
ν_9^{II}	1496 (5)					3.0
ν_{25}	1506		NH_2 b[c]	1.4	1.4	0.6
ν_{26}	1528		C−NH_2 b, C−C st[c]	1.9	2.5	4.3
ν_{27}	1542		NH_2 b[c]	1.5	2.0	5.3
ν_{10}^{II}	1588 (5)					3.3
ν_{28}	1606		NH_2 b[c]	1.7	1.7	3.2
ν_{29}	1630		$\nu_{11} + \nu_{12}$	4.5	4.5	3.4
ν_{30}	1711		2 ν_{12}	2.4	2.9	
ν_{31}	3257		ν_{12} + 2 ν_{17}	9.1	6.5	3.4
ν_{32}	3299		s NH_2 st[c]	−1.6	−1.1	−2.7

dx.doi.org/10.1021/jp5052062 | J. Phys. Chem. A 2014, 118, 5002−5012

Table 1. continued

mode	freq at 1 atm or at the transition: this work (cm^{-1})	freq at 1 atm or at the transition: ref. (cm^{-1})	tent. vibr. assign.	$d\nu/dp$ (cm^{-1} GPa^{-1}): α (1 atm)	$d\nu/dp$ (cm^{-1} GPa^{-1}): I (2 GPa)	$d\nu/dp$ (cm^{-1} GPa^{-1}): II (5 GPa)
ν_{33}	3327		$\nu_{11} + \nu_{17} + \nu_{20}$	−4.4	−4.4	2.6
ν_{34}	3333		s NH_2 st[c]	2.2	−1.1	0.7
ν_{35}	3405		as NH_2 st[c]	−2.6	−1.8	−0.7
ν_{36}	3425		as NH_2 st[c]	−2.0	−1.0	0.9

[a]Modes that occur at 2 or 5 GPa are denoted with superscript I or II, respectively. Abbreviations: il, in-layer; ool, out-of-layer; s, symmetric; as, asymmetric; st, stretching; w, wagging; b, bending; and r, rocking. Note the values of $d\nu/dp$ are not given in table if the mode was not observed at the specific pressure. [b]Ref 20. [c]Ref 27.

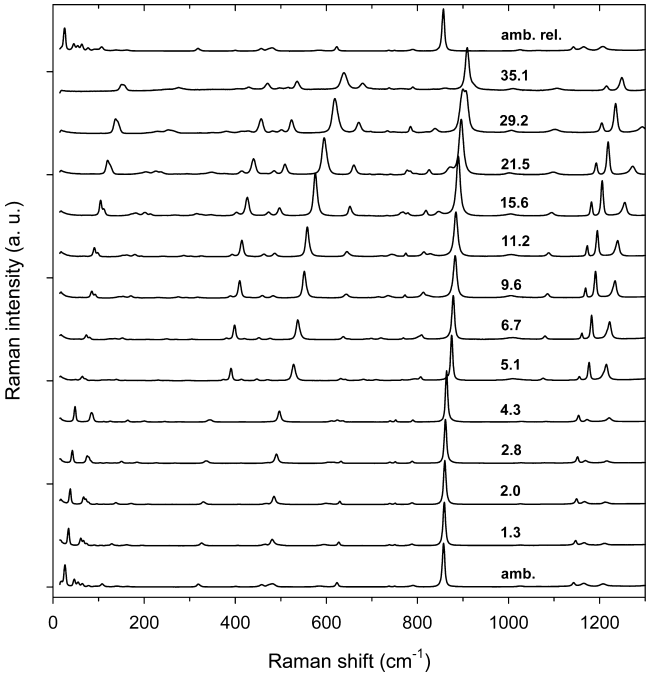

Figure 3. Raman spectra of FOX-7 crystal at several pressures in the frequency range from 0 to 1300 cm^{-1}. Pressure values are given in GPa next to each spectrum. The intensities of spectra at and above 5.1 GPa were multiplied by 2. The top spectrum was measured at ambient pressure after release of pressure from 40 GPa. Note the spectra were obtained with the laser beam parallel to the *b*-axis of the crystal.

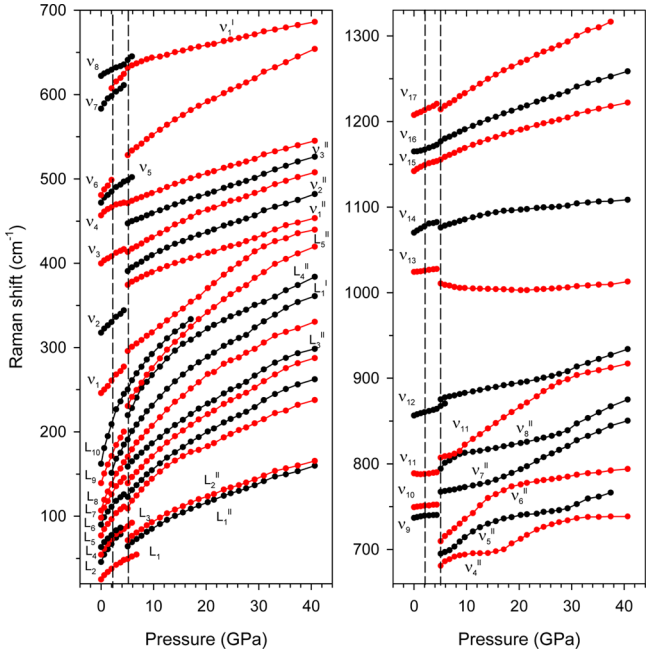

Figure 4. Pressure-induced shifts of Raman peaks in the frequency range from 0 to 1300 cm^{-1}. Experimental results represented by solid points are connected with lines to guide the eye. Two colors are used alternately to distinguish between shifts of different modes. The vertical dashed lines denote pressures for which discontinuities in the Raman peaks shift are observed. Tentative assignment of modes can be found in Table 1. In this and other figures representing the Raman shifts, the error bars are comparable to the plotting points. Note that modes ν_{11} and ν_8'' do not cross.

presented in Table 1. In addition to coefficients at ambient pressure, we also show coefficients at 2 and 5 GPa. The results at these two pressures provide evidence for discontinuities of several modes and indicate potential phase transitions at 2 and 4.5 GPa. Details of these changes are discussed in Section 3.3.

As indicated above, the lattice modes, on average, show pressure coefficients larger than those of the internal modes. Because of this difference, the separation between internal and lattice modes, represented by frequencies of the ν_1 and L_9 modes, reduces from 84 cm^{-1} at ambient pressure to 17 cm^{-1} at 17 GPa. The values of pressure coefficients also varied considerably among the lattice and the internal modes. For example, the differences in pressure shifts between the L_2, L_3, and L_4 modes cause these well-separated peaks at ambient pressure to essentially merge into one peak at 4.3 GPa (see Figures 3 and 4). The difference in pressure shifts also has significant effect on the behavior of internal modes, as discussed in Section 3.4.

As shown in Figure 5, changes in the Raman spectra were accompanied by changes in the crystal appearance and color. The initially yellow crystal transformed instantaneously around 5.1 GPa to a less transparent crystal, with a greyish appearance. With further pressure increase, the greyish appearance intensified, likely due to the formation of plane or line defects in the crystal in a direction normal to the *b*-axis. At pressures higher than 20 GPa, the crystal became reddish-brownish and visible changes in the pressure-transmitting medium were noted. The latter were likely associated with the phase change in nitrogen from the δ to ε at ~18 GPa.[29] The changes in crystal appearance and color were also accompanied by an increase in intensities of selected Raman peaks (see Figure 3). Thus, the observed increase in Raman intensity for pressures to ~30 GPa could result from resonance effects due to favorable changes in the crystal electronic structure. On the other hand, an intensity decrease and broadening of Raman peaks above 30 GPa were likely caused by the increasing role of nonhydrostatic compression effects.

3.2.2. Frequency Range 1350–1700 cm^{-1} (Contributions from the C–N and C–C Stretching and NH_2 Bending Vibrations). Intensities of the Raman peaks in this range are

dx.doi.org/10.1021/jp5052062 | J. Phys. Chem. A 2014, 118, 5002–5012

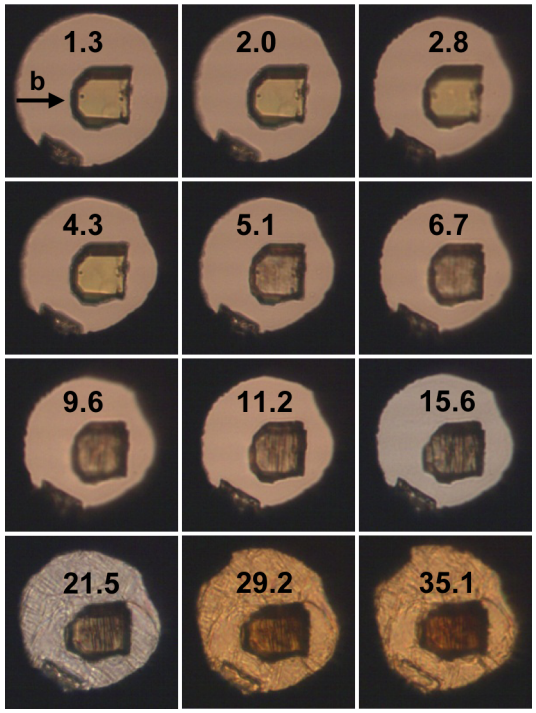

Figure 5. Images of FOX-7 crystal at several pressures in a diamond anvil cell. The images correspond to spectra shown in Figure 3. The diameter of the high-pressure compartment is ~100 μm.

quite low, and relative intensities of peaks depend strongly on the crystal orientation (see Figure 2). Thus, to examine all possible modes in this range, we performed measurements for both orientations. The Raman spectra for crystals oriented with the *b*-axis perpendicular and parallel to the laser beam are shown in Figure S1 of Supporting Information. With increasing pressure, there was noticeable change in the spectra above 4.4 GPa and broadening of peaks with further increase of pressure. The changes in the spectra were also evident from the pressure dependence of the Raman shifts obtained from the combined results for the two orientations. As seen in Figure S2 of Supporting Information, there are clear discontinuities in the shifts of many modes around 4.5 GPa. Also, some peaks, ν_{20}, ν_{21}, and ν_{30}, disappeared at this pressure. While the last two modes had very low intensity at ambient pressure, the ν_{20} mode was the most intense peak in this range, with an intensity that was more than 1 order of magnitude higher than the intensities of the other peaks. Because this mode represents mostly the contributions from the C−NO_2 stretching vibrations, its disappearance (see inset in Figure S1 of Supporting Information) could indicate substantial modifications in the C−N bonding at 4.5 GPa.

3.2.3. Hydrogen Bonding: Frequency Range 3250−3450 cm^{-1} (Contribution from the NH_2 Stretching Vibrations). The ambient structure of FOX-7 is maintained because of the extensive network of intermolecular hydrogen bonds, which cause the layered crystal structure.[2] Thus, the behavior of hydrogen bonding under high pressure is of special interest because it can provide insight into the stability of this crystal at extreme conditions. Changes in the hydrogen bonding can be examined by monitoring changes in the NH_2 stretching vibrations. In FOX-7, there are four NH_2 stretching vibrations: two symmetric, 3299 and 3333 cm^{-1}, and two asymmetric, 3405 and 3425 cm^{-1}. All these vibrations are observed in the spectrum obtained from a crystal excited with a laser beam parallel to the crystal *b*-axis. As shown in Figure 6, increasing

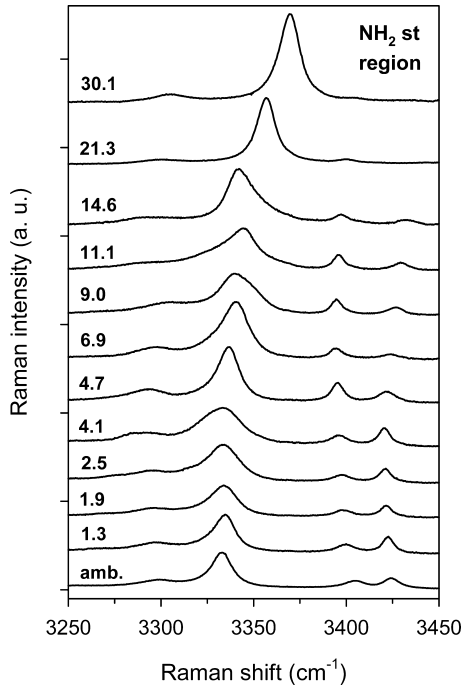

Figure 6. Raman spectra of FOX-7 crystal at several pressures in the frequency range from 3250 to 3450 cm^{-1}. Pressure values are given in GPa next to each spectrum. The intensities of spectra shown at 21.3 and 30.1 GPa were divided by 2.

pressure causes an evolution in the hydrogen bonding network: changes in peak shape, position, and intensity. For example, there is a clear reversal in intensity between the two asymmetric modes at pressures between 4.1 and 4.7 GPa. Furthermore, similar to low-frequency modes, the intensity of selected NH_2 modes increases significantly with pressure. We note that intensities of the spectra at 21.3 and 30.1 GPa, in Figure 6, were reduced by 2 to accommodate the graph.

In Figure S3 of Supporting Information and Figure 7, we show some details regarding the pressure effects on NH_2

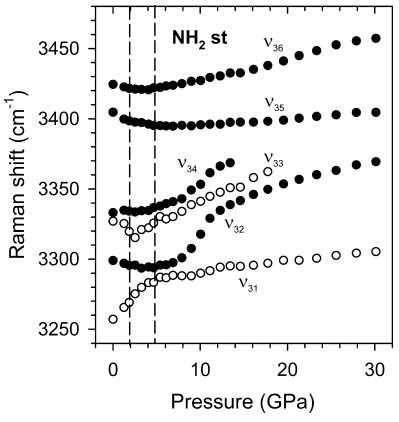

Figure 7. Pressure-induced shifts of Raman peaks in the frequency range from 3250 to 3450 cm^{-1}. Open circles denote peaks assigned to the combination modes. The vertical dashed lines denote pressures for which chages in the Raman peaks shift are observed. Tentative assignment of modes can be found in Table 1.

dx.doi.org/10.1021/jp5052062 | J. Phys. Chem. A 2014, 118, 5002−5012

stretching vibrations. First, we analyzed the complex spectral changes in the range of symmetric vibrations modes. As shown in Figure S3 of Supporting Information, the fitting of spectra in this range requires the use of four peaks rather than two. The additional two peaks appeared at 3257 and 3327 cm^{-1} and were assigned to be combination of modes. Thus, the complex changes in the spectra shape in the range of 3250−3400 cm^{-1} may result from the coupling and mixing between the symmetric NH_2 stretching modes and two combination modes. As seen in Figure S3 of Supporting Information and Figure 7, there is no crossing of those four peaks as pressure increases. Interestingly, the spectrum in this range transforms gradually to two well-separated peaks, with significantly different intensities at high pressures. The two peaks were associated with the NH_2 stretching vibrations, an intense peak, and with the combination vibrations, a weak peak. It is known that hydrogen bonding is highly anisotropic in FOX-7 at ambient conditions; the H-bonds are shorter and the interactions are likely stronger between the molecules within the "bands" than between the molecules belonging to different bands (see Figure 1b). Thus, the presence of intense and relatively narrow peaks for the NH_2 stretching vibrations suggests ordering of the ambient anisotropic H-bonding network at high pressures.

Pressure effects on the frequencies of the Raman peaks in the region of NH_2 stretching vibrations are shown in Figure 7. Frequencies of both the symmetric and asymmetric NH_2 modes decrease with the initial pressure increase; this behavior can be attributed to the strengthening of hydrogen bonding. However, at higher pressures, there is gradual change in the direction of these shifts. The turning pressure for this change coincides approximately with discontinuities observed in many other modes at 4.5 GPa (e.g., Figure 4) as well as with the increase in coupling between the symmetric NH_2 and the combination modes. Thus, the increase in frequency of NH_2 stretching vibrations at higher pressures appears to result from the crystal structural changes occurring at 4.5 GPa. A steep increase in frequency of two symmetric vibrations, ν_{32} and ν_{34}, after the phase transition suggests a substantial softening of the hydrogen bonding network at higher pressures.

3.3. High-Pressure Polymorphs of FOX-7. The Raman results presented above indicated spectral changes around 2 and 4.5 GPa, potentially due to phase transformations in FOX-7 at these pressures. Here, we discuss possible structural effects related to the observed spectral changes. The phases above 2 and 4.5 GPa are tentatively labeled as I and II.

3.3.1. High-Pressure Phase-I. Only a limited number of modes were affected around 2 GPa. The main changes involved a low-frequency range, in which a couple of peaks showed up and one vanished. This can be seen in Figure 8, as we compare, side-by-side, Raman spectra obtained just below and above 2 GPa. The changes include two peaks that emerged at ∼151 cm^{-1} (L_1') and 607 cm^{-1} (ν_1'), and one shoulder that disappeared at 499 cm^{-1} (ν_6). Also, a few modes, ν_{11}, ν_{14}, and ν_{33}, showed noticeable changes in pressure shift around 2 GPa. The shift turned from red to blue for the ν_{11} and ν_{33} modes, while the slope changed for the ν_{14} mode. All of the above changes were reproducible in various pressure media and were reversible at the same pressure (∼2 GPa) upon unloading from high pressures. The limited extent of these changes implies fairly minor modifications to the FOX-7 structure. Because the changes in the lattice modes were very minimal, only a small peak showed up at 151 cm^{-1}, it is unlikely that structural

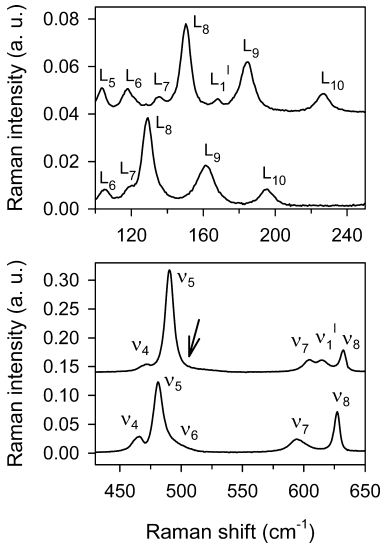

Figure 8. Raman spectra of FOX-7 crystal in two different frequency ranges obtained below and above 2 GPa; the bottom spectrum was obtained at 1.5 GPa, whereas the top spectrum at 2.6 GPa. Arrow indicates the disappearance of mode ν_6. The mode assignments can be found in Table 1.

modifications at 2 GPa involve the crystal structure (crystal system and/or space group). Instead, it seems that the changes likely involve alteration of the molecular conformation. Single-crystal X-ray diffraction experiments are underway to determine the structure above 2 GPa.

3.3.2. High-Pressure Phase-II. The spectral changes at 4.5 GPa are very extensive. They include substantial changes in both the lattice and internal vibrations. In Figure 9, we compare side by side the spectra obtained at 4.3 and 5.1 GPa in selected frequency ranges. In the range of lattice modes (Figure 9a), two well-separated peaks transformed to two overlapped peaks. Note that at 4.3 GPa, the second peak is a combination of three modes, L_2−L_4. We also notice that small peaks outside of L_1'' and L_2'' modes are the leftovers from the spectrum of 4.3 GPa. The presence of these peaks at pressures above 4.5 GPa indicates that the transformation was not fully completed at the transition. This behavior was also observed for a few other modes. However, all these peaks disappeared with further increase of pressure to 6−7 GPa (see Figure 4).

The differences in the internal modes below and above the transition are illustrated in Figure 9b−d. They include (i) the occurrence of new peaks, ν_1''-ν_3'', (panel b); (ii) the exchange of intensities between ν_{15}, ν_{16}, and ν_{17} modes (panel c); and (iii) the disappearance of strong C−NO_2 stretching mode, ν_{20}, (panel d). In addition, there were significant changes in the pressure shifts. A close examination of Figure 4 reveals that the modes associated with the out-of-layer vibrations, ν_1, ν_2, ν_8, ν_9, and ν_{10}, either disappeared or significantly shifted at the transition. On the other hand, the in-layer vibrations, ν_3, ν_4, ν_{13}, and ν_{14}, were generally much less affected at the transition. This observation suggests that the phase change at 4.5 GPa could be driven by a change in the balance between the interlayer and in-layer interactions.

At ambient conditions, the interactions between the layers are weak (van der Waals), while the interactions within the layers are relatively strong (H-bonding). With increasing pressure to 4.5 GPa, the hydrogen bonding strength further increases forming stronger in-layer bonds, as concluded from

dx.doi.org/10.1021/jp5052062 | J. Phys. Chem. A 2014, 118, 5002−5012

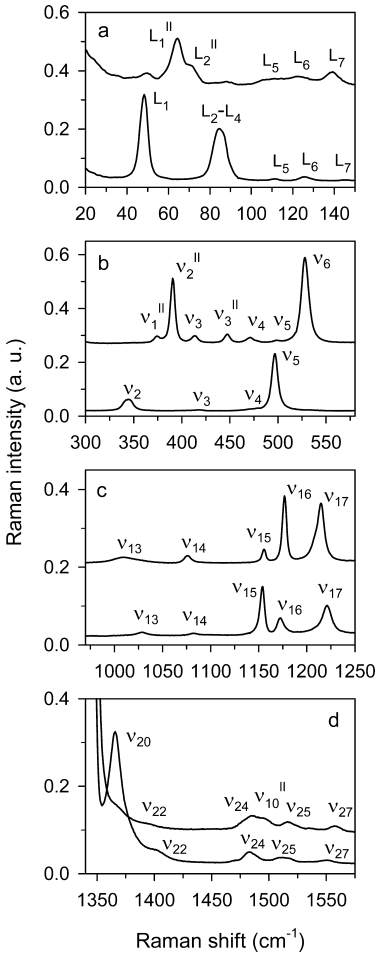

Figure 9. Raman spectra of FOX-7 crystal in different frequency ranges obtained below and above 4.5 GPa; the bottom spectrum was obtained at 4.3 GPa, whereas the top spectrum at 5.1 GPa. The intensities of spectra at 5.1 GPa were multiplied by 4 (panel a) and by 2 (panels b and d). The mode assignments can be found in Table 1.

the results in Figure 7. At the same time, the interactions between the layers increase substantially as the interlayer distance decreases considerably because of the initially large compressibility in the direction normal to the layers.[20] Seemingly, at 4.5 GPa, the layers approach the distance that intramolecular strains no longer support the increase of repulsive contribution to the total energy. Thus, the phase transition is expected to relieve the repulsive interactions between the layers, for example, by a concerted modification of wave-shaped layers and rearrangement of molecules in the layer. Significant changes in both the lattice and intramolecular modes at 4.5 GPa imply that the conjectured structural changes involve both molecular and crystal transformations. Because the pressure shifts of NH_2 stretching modes change gradually from red to blue around 4.5 GPa, it seems that the phase transition preserves the hydrogen bonding network.

Another piece of information regarding the phase transition at 4.5 GPa can be obtained from the unloading experiments. As shown in Figure 10, the crystal compression beyond 30 GPa and subsequent gradual unloading of pressure demonstrate that the changes observed at 4.5 GPa (during loading) display considerable hysteresis during unloading. The high-pressure phase (phase-II) persisted down to ~1.0 GPa, indicating its metastable character over a broad range of pressure. This large

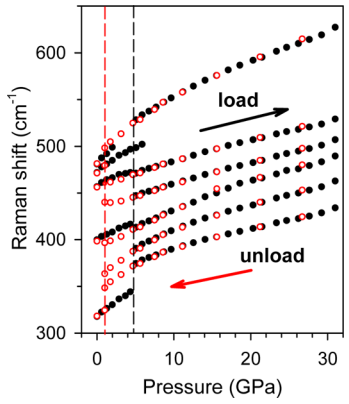

Figure 10. Comparison of pressure effects on Raman shifts upon loading (solid points) and unloading (red circles) the pressure. The vertical dashed lines denote the pressures for which discontinuities in the Raman peaks shift are observed: black line (loading) and red line (unloading).

hysteresis suggests a reconstructive character of the phase-I-to-phase-II transformation. We note that phase-I was not observed upon unloading from phase-II. Instead, the crystal transformed directly to the α-phase below 1.0 GPa.

We also found that the pressure onset for the phase-I-to-phase-II transition depends on the pressure-transmitting medium. The results were very similar in nitrogen, methanol/ethanol mixture, and neon, whereas they were different in argon. To demonstrate this, we compare the pressure effect on the evolution and shift of a strong peak of ν_{12} in nitrogen and argon (Figures 11 and 12). In nitrogen, the intensity of this

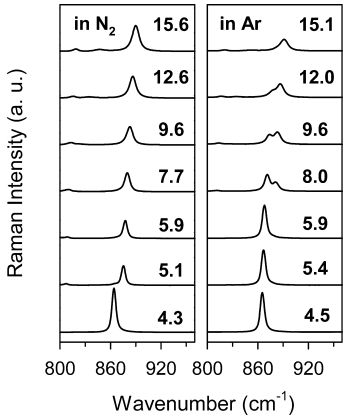

Figure 11. Evolution of Raman peak (ν_{12}, NO and NH rocking vibration) with pressure in two pressure media: nitrogen and argon.

peak decreases and the frequency shifts up by ~11 cm^{-1} at the phase transition. Thus, the onset of transition was clearly observed around 4.5 GPa, and the transition was completed by ~7 GPa, as deduced from a complete disappearance of a low-frequency peak. However, in argon, the changes in the ν_{12} peak started at ~6 GPa and progressed over a broad range of pressures. The results (for argon) in Figures 11 and 12 show that the two peaks coexist at several pressures and the intensity of the high-frequency peak increases at the expense of the low-frequency peak with increasing pressure. This coexistence of the two crystal states continued until the transformation of phase-I to phase-II was completed by ~14 GPa. Also, the peak

dx.doi.org/10.1021/jp5052062 | J. Phys. Chem. A 2014, 118, 5002−5012

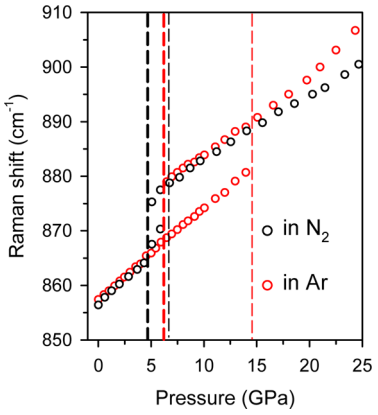

Figure 12. Pressure shift of ν_{12} peak in nitrogen (black circles) and argon (red circles). The black and red vertical, thick-dashed lines denote the pressures for the onset of phase transformations in nitrogen and argon medium, respectively, while the thin-dashed lines for the completion of transformations.

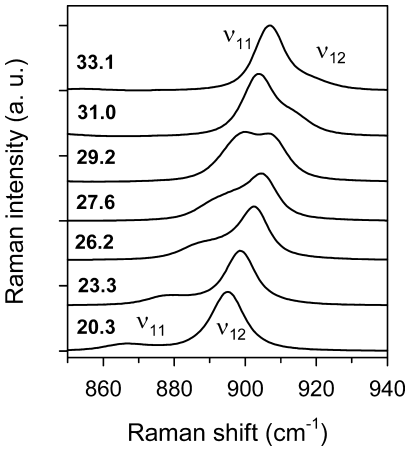

Figure 13. Evolution of Raman spectra at several pressures to illustrate coupling between the ν_{11} and ν_{12} modes.

shifts in argon and nitrogen deviated somewhat from each other above the phase transition (Figure 12).

It has been reported that argon, in contrast to the other media used in this work, can develop pressure gradients at relatively low pressures.[30] By using ruby spheres equally distributed in the pressure chamber, it was found that the average distribution of pressure in argon was 0.05 at 5 GPa. Therefore, different behavior of FOX-7 in argon, as represented by the higher transition pressure, the coexistence of two phases over a large range of pressure, and the different pressure shifts, can be attributed to nonhydrostatic effects. This conclusion is consistent with the fact that we observed a shortening of the pressure range for the coexistence of two phases by using smaller crystals. Lastly, the results in argon show that the behavior of FOX-7 at high pressures can be affected by pressure gradients, even as small as 0.05 GPa. This could be one of the reasons that previous studies on FOX-7 without[19,20] or with solid[21,22] pressure-transmitting media reported contradicting responses and different transition pressures.

3.4. Coupling of Modes. Our results indicate several instances of intensity exchange between various modes with increasing pressure. In each case, this behavior was observed between two different modes, either both fundamental or fundamental and combination/overtone, and having very different intensities initially. Examples of these modes include: $\nu_1-\nu_1''$, $\nu_4''-\nu_5''$, $\nu_6''-\nu_7''$, $\nu_8''-\nu_{11}$, $\nu_{11}-\nu_{12}$, $\nu_{31}-\nu_{32}$, and $\nu_{33}-\nu_{34}$. We have attempted to model this apparent coupling between different vibrations using the Fermi resonance model. We use changes in ν_{11} (C−NO_2 rocking) and ν_{12} (NO and NH rocking) modes as an example. The spectral evolution and frequency shifts of these two modes with pressure are presented in Figures 13 and 14a, respectively. As seen, the initially low-intensity ν_{11} mode is gaining intensity while shifting with pressure to higher frequency. Above ∼28 GPa, the intensity exchange and the avoided frequency crossing between the two modes is clearly observed.

The phenomenon of Fermi resonance (FR) is quite common in complex molecules. However, it has not been reported in energetic solids, until recently.[31] Fermi resonance occurs when two molecular vibrational modes of the same symmetry are perturbed by the anharmonic term in the Hamiltonian describing the system.[32,33] As a result, the energy levels of both vibrations are changed and mixed, leading to changes in

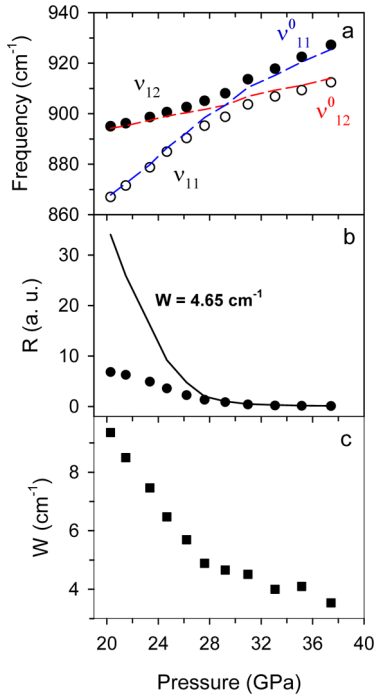

Figure 14. Details of pressure effect on modes ν_{11} and ν_{12} described within the Fermi resonance framework. (a) Raman frequencies; experimental data (solid and open circles) and anticipated shifts without the coupling, dashed blue and red lines, calculated from eq 7. (b) Raman modes intensity ratio; experimental data (solid points) and calculated from eq 5 for $W = 4.65$ cm^{-1}. (c) Pressure dependence of W obtained from eq 6

the observed frequencies and intensity transfer from one mode to the other. Thus, the experimental observables in FR are the frequency separation between the peaks, δ, and the ratio of the intensity of the modes, R.

A relation between the observed, ν^+ and ν^-, and the unperturbed frequencies (with no resonance), ν_0^+ and ν_0^-, may be obtained from a two-level perturbative analyses.[32,33] In this framework, the frequency separation between the observed modes, $\delta = \nu^+ - \nu^-$, is related to the unperturbed frequency separation, $\delta_0 = \nu_0^+ - \nu_0^-$, by the following relation:[33]

$$\delta^2 = \delta_0^2 + 4W^2 \quad (1)$$

dx.doi.org/10.1021/jp5052062 | J. Phys. Chem. A 2014, 118, 5002−5012

where W is the Fermi resonance coefficient, which defines the coupling strength between the two modes.

The observed intensity ratio of the coupled modes, $R = I_+/I_-$, can be expressed in terms of δ, δ_0, and the hypothetical mode intensity ratio in the absence of Fermi resonance, R_0:[33]

$$R = \frac{I_+}{I_-} = \left[\frac{(\delta + \delta_0)^{1/2}R_0^{1/2} + (\delta - \delta_0)^{1/2}}{(\delta - \delta_0)^{1/2}R_0^{1/2} - (\delta + \delta_0)^{1/2}}\right]^2 \quad (2)$$

At exact resonance (degeneracy) of two unperturbed modes, i.e., for $\delta_0 = 0$, eqs 1 and 2 transform to

$$\delta = 2W \quad (3)$$

and

$$R = \left[\frac{R_0^{1/2} + 1}{R_0^{1/2} - 1}\right]^2 \quad (4)$$

thus allowing the direct determination of W and R_0 from the experimental frequencies and intensities. From the results shown in Figure 14a, we estimate $W = 4.65 \pm 0.5$ cm^{-1}; from the results in Figure 14b, we find that the intensity ratio reaches a value of ~0.95 at the minimum of δ. Hence, from eq 4, the R_0 is found $\sim 6 \times 10^3$. This large value of R_0 justifies the approximation of eq 2 by a simplified form:

$$R = \frac{\delta + \delta_0}{\delta - \delta_0} \quad (5)$$

Equation 5 in combination with eq 1 was used to validate the applicability of the model to our data. The results obtained from eq 5, with the constant value of $W = 4.65$ cm^{-1}, for all pressures are plotted in Figure 14b. It is clear that the model gives an intensity ratio at lower pressures much larger than that observed experimentally.

One possible contribution to this discrepancy could be the assumption of constant value of W with pressure. Though such an assumption is often made,[31] it has been shown that W can change considerably with pressure.[34] Thus, an alternate approach may be used. By combining eqs 5 and 1, for a given set of experimental R and δ values determined over a range of pressures, the equation

$$W = \frac{\delta R^{1/2}}{R + 1} \quad (6)$$

may be used to determine the pressure dependence of W (if any). The results from eq 6 are plotted in Figure 14c and show changes in W with pressure. Thus, this result implies that the Fermi resonance coupling parameter between the ν_{11} and ν_{12} modes may be pressure-dependent. Using the pressure dependence of W, the unperturbed frequencies were calculated from the relation

$$|\nu_+ - \nu_+^0| = |\nu_- - \nu_-^0| = (\delta - \delta_0)/2 \quad (7)$$

and plotted in Figure 14a.

The above considerations indicate that interaction between the ν_{11} and ν_{12} modes may be described in terms of Fermi resonance by using a pressure-dependent coupling parameter. We found that the description of coupling of other interacting modes, e.g., ν_1–ν_1'' and ν_{31}–ν_{32} also requires W to be pressure-dependent; this attribute appears to be a characteristic for the FOX-7 behavior under high pressures.

Finally, the observed substantial coupling or mixing between the different modes at various pressures may have some implication for the shock insensitivity of FOX-7. Although the molecular mechanism for shock initiation of FOX-7 is unknown, it is often anticipated that the C–NO_2 bond homolysis could be an important step in the decomposition process.[6,35] The coupling between the C–NO_2 and NH vibrations, represented by the interaction of ν_{11}–ν_{12}, ν_{31}–ν_{32}, and ν_{33}–ν_{34} modes, observed in our work suggests that energy cannot be easily localized in C–N motions under high pressure. It is likely delocalized between the C–N and N–H bonding vibrations. In effect, the energy from the shock wave imparted to the crystal could be shared between the C–N and N–H bonds, thus requiring higher stresses or energies for the crystal to be initiated. This proposed energy transfer between the C–N and N–H bonds and the demonstrated stability of the Raman spectra at high pressures provide potential molecular insights into the shock insensitivity of FOX-7.

4. SUMMARY AND CONCLUSIONS

We carried out comprehensive Raman measurements on FOX-7 single crystals over the entire frequency range of Raman activities and over a broad pressure range. The results of this work provide pressure dependence of the lattice and intramolecular modes and, in particular, clear evidence for spectral changes at 2 and 4.5 GPa. These changes were proposed to be associated with the following phase transitions: a molecular conformational change at 2 GPa and molecular/crystal changes at 4.5 GPa. The pressure hysteresis observed for the spectral changes at 4.5 GPa was associated with the reconstructive character of the transformation at this pressure. Also, the Raman data suggested that this transformation reflects a change in the balance between the interlayer and in-layer molecular interactions. Despite these two transformations, the spectra were fully reversible upon the release of pressure from 40 GPa, implying remarkable chemical stability of FOX-7 over a large pressure range.

Changes in the NH_2 stretching vibrations indicated the strengthening of hydrogen bonds with pressure increase to 4.5 GPa. However, further increase of pressure led to an apparent ordering of the hydrogen bonding network. We also observed several instances of substantial coupling or mixing between the different vibrational modes at various pressures. This behavior was analyzed within the framework of the Fermi resonance model; the experimental data show the Fermi resonance coupling parameter to be pressure-dependent. Finally, we propose that the observed vibrational coupling between the different modes, particularly between the C–N and N–H modes, may have implications for the shock insensitivity of FOX-7.

■ ASSOCIATED CONTENT

Supporting Information

Raman spectra and pressure-induced shifts of Raman peaks in the frequency range from 1350 to 1750 cm^{-1} (Figures S1 and S2, respectively); Raman spectra deconvolution to four peaks in the frequency range from 3260 to 3380 cm^{-1} (Figure S3). This material is available free of charge via the Internet at http://pubs.acs.org.

■ AUTHOR INFORMATION

Corresponding Author

*E-mail: dreger@wsu.edu, phone: 509-335-4233.

Notes

The authors declare no competing financial interest.

■ ACKNOWLEDGMENTS

Dr. Joel R. Carney from Naval Surface Warfare Center-Indian Head Division (NSWC-IHD) is thanked for providing the FOX-7 powder. This work was supported by Department of Energy National Nuclear Security Administration (DOE/NNSA) Grant DE-NA0000970 and Office of Naval Research (ONR) Grant N000014-12-1-0555.

■ REFERENCES

(1) Latypov, N. V.; Bergman, J.; Langlet, A.; Wellmar, U.; Bemm, U. Synthesis and Reactions of 1,1-diamino-2,2-dinitroethylene. *Tetrahedron* **1998**, *54*, 11525−11536.

(2) Bemm, U.; Östmark, H. 1,1-Diamino-2,2-Dinitroethylene: A Novel Energetic Material with Infinite Layers in Two Dimensions. *Acta Crystallogr., Sect. C: Cryst. Struct. Commun.* **1998**, *54*, 1997−1999.

(3) Lochert, I. J. *FOX-7 - A New Insensitive Explosive*. DSTO-TR-1238; Defence Science and Technology Organization, Aeronautical and Maritime Research Laboratory: Victoria, Australia, 2001;pp 1−23.

(4) Östmark, H.; Bergman, H.; Bemm, U.; Goede, P.; Holmgren, E.; Johansson, M.; Langlet, A.; Latypov, N.; Pettersson, A.; Pettersson, M. L.; et al. 2,2-Dinitroethene-1,1-Diamine (FOX-7) - Properties, Analysis, and Scale Up. *Proc. 32nd ICT Int. Annu. Conf. on Energy Mater.*, Vol. *26*, Karlsruhe, Germany, July 4−7, 2001.

(5) Anniyappan, M.; Talawar, M. B.; Gore, G. M.; Venugopalan, S.; Gandhe, B. R. Synthesis, Characterization and Thermolysis of 1,1-Diamino-2,2-dinitroethylene (FOX-7) and Its Salts. *J. Hazard. Mater.* **2006**, *137*, 812−819.

(6) Bellamy, A. J. In *Structrure and Bonding*; Mingos, D. M., Ed.; Springer-Verlag: Berlin, 2007; Vol. *125*, pp 1−33.

(7) Daniel, M. A.; Davies, P. J.; Lochert, I. J. *FOX-7 for Insensitive Boosters*. DSTO-TR-2449; Defence Science and Technology Organization, Aeronautical and Maritime Research Laboratory: Edinburgh, Australia, 2010; pp 1−18.

(8) Cullis, I. G.; Townsley, R. The Potential of FOX-7 Explosive in Insensitive Munition Design. *J. Appl. Mech.* **2011**, *78*, 051012.

(9) Mathieu, D. Theoretical Shock Sensitivity Index for Explosives. *J. Phys. Chem. A* **2012**, *116*, 1794−1800.

(10) Hooper, J. Vibrational Energy Transfer in Shocked Molecular Crystals. *J. Chem. Phys.* **2010**, *132*, 014507.

(11) Baer, B. J.; Oxley, J.; Nicol, M. Raman Spectroscopy of High Explosives at High Pressures used to Detect Phase Transition of RDX (Hexahydro-1,3,5-Trinitro-s-Triazine. *High Pressure Res.* **1990**, *2*, 99−108.

(12) Dreger, Z. A.; Gupta, Y. M. High Pressure Raman Spectroscopy of Single Crystals of Hexahydro-1,3,5-trinitro-1,3,5-triazine (RDX). *J. Phys. Chem. B* **2007**, *111*, 3893−3903.

(13) Patterson, J. E.; Dreger, Z. A.; Gupta, Y. M. Shock Wave-Induced Phase Transition in RDX Single Crystals. *J. Phys. Chem. B* **2007**, *111*, 10897−10904.

(14) Dreger, Z. A.; Gupta, Y. M. Raman Spectroscopy of High-Pressure−High-Temperature Polymorph of Hexahydro-1,3,5-trinitro-1,3,5-triazine (ε-RDX). *J. Phys. Chem. A* **2010**, *114*, 7038−7047.

(15) Dreger, Z. A.; Gupta, Y. M. Phase Diagram of Hexahydro-1,3,5-trinitro-1,3,5-triazine Crystals at High Pressures and Temperatures. *J. Phys. Chem. A* **2010**, *114*, 8099−8105.

(16) Kempa, P. B.; Herrmann, M. Temperature Resolved X-ray Diffraction for the Investigation of the Phase Transitions of FOX-7. *Part. Part. Syst. Char.* **2005**, *22*, 418−422.

(17) Evers, J.; Klapötke, T. M.; Mayer, P.; Oehlinger, G.; Welch, J. α- and β-FOX-7, Polymorphs of a High Energy Density Material, Studied by X-ray Single Crystal and Powder Investigations in the Temperature Range from 200 to 423 K. *Inorg. Chem.* **2006**, *45*, 4996−5007.

(18) Crawford, M.-J.; Evers, J.; Goebel, M.; Klapoetke, T. M.; Mayer, P.; Oehlinger, G.; Welch, J. M. Gamma-FOX-7: Structure of a High Energy Density Material Immediately Prior to Decomposition. *Propellants, Explos., Pyrotech.* **2007**, *32*, 478−495.

(19) Peiris, S. M.; Wong, C. P.; Kuklja, M. M.; Zerilli, F. J.Equation of State and Structural Changes in Diaminodinitroethylene from Experimental Studies and Ab-Initio Quantum Calculations. In *Proceedings of 12th International Detonation Symposium*, San Diego, CA, August 11−16, 2002; pp 617−624.

(20) Peiris, S. M.; Wong, C. P.; Zerilli, F. J. Equation of State and Structural Changes in Diaminodinitroethylene under Compression. *J. Chem. Phys.* **2004**, *120*, 8060−8066.

(21) Pravica, M.; Liu, Y.; Robinson, J.; Velisavljevic, N.; Liu, Z. X.; Galley, M. A. High-Pressure Far- and Mid-Infrared Study of 1,1-diamino-2,2-dinitroethylene. *J. Appl. Phys.* **2012**, *111*, 103534−9.

(22) Bishop, M. M.; Chellappa, R. S.; Pravica, M.; Coe, J.; Liu, Z.; Dattlebaum, D.; Vohra, Y.; Velisavljevic, N. 1,1-diamino-2,2-dinitroethylene under High Pressure-Temperature. *J. Chem. Phys.* **2012**, *137*, 174304−8.

(23) Dreger, Z. A.; Tao, Y.; Gupta, Y. M. Polymorphs of 1,1-diamino-2,2-dinitroethene (FOX-7): Isothermal Compression Versus Isobaric Heating. *Chem. Phys. Lett.* **2013**, *584*, 83−87.

(24) Hu, A.; Larade, B.; Goebel, M.; Abou-Rachid, H.; Lussier, L.-S. A First Principles Density Functional Study of Crystalline FOX-7 Chemical Decomposition Process under External Pressure. *Propellants, Explos., Pyrotech.* **2006**, *5*, 355−360.

(25) Wu, Q.; Zhu, W.; Xiao, H. DFT Study on Crystalline 1,1-diamino-2,2-dinitroethylene Under High Pressure. *J. Mol. Model.* **2013**, *19*, 4039−4047.

(26) Park, T.-R.; Dreger, Z. A.; Gupta, Y. M. Raman Spectroscopy of Pentaerythritol Single Crystals under High Pressures. *J. Phys. Chem. B* **2004**, *108*, 3174−3184.

(27) Sorescu, D. C.; Boatz, J. A.; Thompson, D. L. Classical and Quantum-Mechanical Studies of Crystalline FOX-7 (1,1-diamino-2,2-dinitroethylene). *J. Phys. Chem. A* **2001**, *105*, 5010−5021.

(28) Zallen, R.; Slade, M. L. Influence of Pressure and Temperature on Phonons in Molecular Chalcogenides: Crystalline As_4S_4 and S_4N_4. *Phys. Rev. B: Condens. Matter Mater. Phys.* **1978**, *18*, 5775−5798.

(29) Westerhoff, T.; Wittig, A.; Feile, R. High-Pressure Raman Scattering of the Stretching Mode in Nitrogen Along the 300 K Isotherm. *Phys. Rev. B: Condens. Matter Mater. Phys.* **1996**, *54*, 14−17.

(30) Klotz, S.; Chervin, J.-C.; Munsch, P.; Marchand, G. L. Hydrostatic limits of 11 Pressure Transmitting Media. *J. Phys. D: Appl. Phys.* **2009**, *42*, 075413−9.

(31) McWilliams, R. S.; Kadry, Y.; Mahmood, M. F.; Goncharov, A. F.; Ciezak-Jenkins, J. Structural and Chemical Properties of the Nitrogen-Rich Energetic Material Triaminoguanidinium 1-methyl-5-nitriminotetrazolate Under Pressure. *J. Chem. Phys.* **2012**, *137*, 054501.

(32) Herzberg, G. *Infrared and Raman Spectra of Polyatomic Molecules*; D. Van Nostrand: New York, 1945.

(33) Bertran, J. F.; Ballester, L.; Dobrihalova, L.; Sánchez, N.; Arrieta, R. Study of Fermi Resonance by the Method of Solvent Variation. *Spectrochim. Acta, Part A* **1968**, *24*, 1765−1776.

(34) Wu, Y. H.; Shimizu, H. High Pressure Raman Study of Liquid and Crystalline CH_3F up to 12 GPa. *J. Chem. Phys.* **1995**, *102*, 1157−1163.

(35) Dorsett, H. *Computational Studies of FOX-7, A New Insensitive Explosive*. DSTO-TR-1054; Defence Science and Technology Organization, Aeronautical and Maritime Research Laboratory: Salisbury, Australia, 2000; pp 1−19.